Passive Metasurface-Based Low Earth Orbit Ground Station Design

Hao Pan* and Lili Qiu

Abstract: Low Earth Orbit (LEO) satellite communication is vital for wireless systems. The main challenges in designing LEO satellite ground stations include increasing the input signal strength to counteract severe path loss, and adaptively steering the direction of the output signal to accommodate the continuous movement of LEO satellites. To overcome these challenges, we present a novel transceiver system, referred to as MetaLEO. This system integrates a passive metasurface with a small phased array, enabling powerful focusing and adaptive signal steering. By harnessing the metasurface's robust wavefront manipulation capabilities and the programmability of phased arrays, MetaLEO offers an efficient and cost-effective solution that supports both uplink and downlink bands. Specifically, we devise a joint optimization model specifically to obtain the optimal uplink codebook for phased array antennas and metasurface phase profile, which enables electronic steering. In a similar manner, we establish the downlink metasurface phase profile to enhance focusing and signal reception. MetaLEO's efficacy is evaluated via theoretical analysis, simulations, and experiments. Our prototype includes a single metasurface with 21×21 uplink and 22×22 downlink elements, and a 1×4 antenna array for receiving and transmitting. Experimental results show signal strength improvements of 8.32 dB (uplink) and 16.57 dB (downlink).

Key words: Low Earth Orbit (LEO) communication; passive metasurface; phased array antenna

1 Introduction

The importance of Low Earth Orbit (LEO) satellite communication cannot be overstated in today's increasingly interconnected world. As a crucial component of global communication infrastructure, LEO satellite systems have the potential to bridge the digital divide by providing high-speed Internet access to remote and underserved regions that traditional terrestrial networks cannot reach. LEO satellite communication offers several advantages over other forms of satellite systems, such as Geostationary Earth Orbit (GEO) and Medium Earth Orbit (MEO) satellites. With their closer proximity to Earth, LEO

satellites enable lower latency and higher data transfer speed, making them ideal for latency-sensitive applications, like video conferencing, online gaming, and telemedicine.

The decline in costs for launching small, low-orbit satellites has opened up possibilities for widespread LEO satellite technology adoption. Nevertheless, the present bottleneck lies in ground station equipment, as it faces multiple challenges due to LEO satellites' unique characteristics, which need to be tackled to ensure efficient and reliable connectivity. (1) Antenna tracking: LEO satellites move rapidly across the sky, unlike stationary GEO satellites, necessitating constant tracking and antenna orientation adjustments by ground stations to maintain stable communications. This calls for the creation of precise and agile tracking systems, which can be complex, expensive, and power-consuming. (2) Signal strength and interference: The closer distance between LEO satellites and ground

• Hao Pan and Lili Qiu are with Wireless and Networking Research Group, Microsoft Research Asia, Shanghai 200232, China. E-mail: panhao@microsoft.com; liliqiu@microsoft.com.
* To whom correspondence should be addressed.

stations leads to higher frequency signals, making them more susceptible to interference, attenuation, and signal fading. Addressing these challenges requires the design of specialized antennas, filters, and signal processing techniques for ground stations. (3) Scalability and cost: As LEO satellite constellations grow, ground stations need to support an increasing number of satellites while keeping costs and complexity under control. This necessitates the development of scalable and cost-effective solutions capable of steering beams and handling multiple simultaneous connections.

Metasurface technology, enabling precise control over electromagnetic (EM) wavefronts, offers a unique opportunity to redesign the transceiver antenna system in wireless communication networks. Owing to its affordability, compactness, ease of deployment, and passive operation (i.e., no power supply required), metasurface serves as an ideal solution for developing modern and efficient ground station for LEO.

In this study, we introduce an innovative passive metasurface-enhanced LEO ground station system, called MetaLEO, designed to significantly boost uplink and downlink Received Signal Strength (RSS) between ground stations and LEO satellites. Figure 1 shows an example of application scenario of our system. During uplink, MetaLEO directs transmitted EM waves towards one or multiple target satellites in various directions. During downlink, MetaLEO captures EM signals from LEO satellites within its field of view and concentrates them to enhance RSS and throughput. Gateway devices convert LEO network signals (e.g., Ka and Ku bands) into indoor communication network

Fig. 1 Motivation of designing a metasurface-aided low-cost ground station for LEO satellite communications.

signals (e.g., Wi-Fi bands), enabling end-users to seamlessly access LEO services.

While there has been significant progress in metasurface research, several critical challenges must be addressed to implement a practical passive metasurface for LEO satellite communication scenarios. First, LEO satellite communication systems use separate frequency bands for uplink and downlink transmissions to ensure efficient and interference-free communication between ground stations and satellites. This dedicated allocation of distinct frequency bands helps maintain data transmission quality and reliability while minimizing potential signal interference. Consequently, using a single metasurface for both uplink and downlink can reduce costs and save space, but avoiding interference becomes difficult. Second, since transmission antennas and metasurfaces remain stationary while LEO satellites continuously move, it is crucial for the outgoing angle from the metasurface to consistently match satellite movement during uplink communication. The challenge lies in designing a static and passive metasurface capable of dynamically steering EM signals from transmission antennas towards moving LEO satellites, as passive metasurfaces cannot be reconfigured after fabrication. Lastly, for downlink communication, reception antennas are also stationary, and the constant motion of LEO satellites results in a continuously changing angle of incident signal towards the metasurface. The third challenge involves focusing the EM waves passing through the metasurface onto reception antennas, enhancing the received signal strength for all possible incident angles. In summary, our goal is to develop a low-cost, compact LEO transceiver system using metasurface technology, with the following three advantages: (1) a single metasurface supporting both uplink and downlink frequency bands; (2) adaptively directing transmitted signals towards target satellites through software methods; and (3) focusing satellite signals in the downlink across various incident angles to enhance RSS.

We commence the process by developing a metasurface unit cell (or meta-atom) that simultaneously supports downlink (e.g., 20 GHz) and uplink (e.g., 30 GHz) frequencies, while achieving over 90% transmittance and 360-degree phase modulation capability. We design an innovative Huygens metasurface unit by strategically placing the downlink pattern unit at the center and the uplink pattern unit
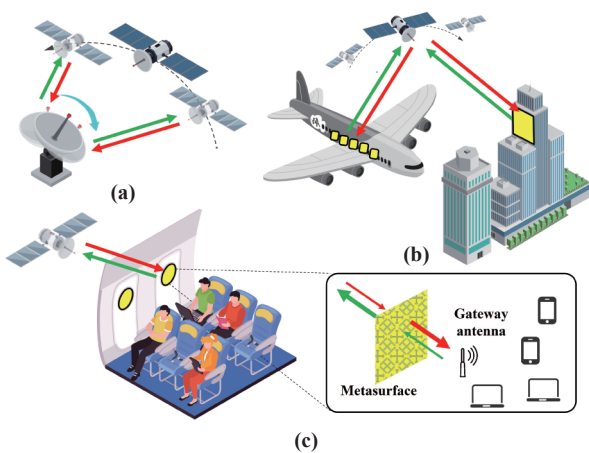
around the corners. To facilitate dynamic functionality for both downlink and uplink, we propose a distinctive integration of a passive metasurface with small-scale phased array transmission/reception antennas. This combination allows our system to enable software-based adaptive steering and focusing. The passive metasurface precisely modulates various EM wave-fronts emitted from the phased array antennas with distinct weights, enabling our system to direct the EM waves originating from the transmission antennas towards target satellites, and concentrate the EM waves from the target satellites towards the reception antennas. We develop a comprehensive channel model for the phased array antennas and metasurface in the uplink and downlink separately, considering the near-field channel response between each antenna and each metasurface element. We then model the optimization problems for the jointly design of the codebook (i.e., phase shift information) and phase compensation map, and utilize a gradient descent-based algorithm to achieve the the optimal configurations. In details, for the uplink, the configuration comprises the optimized phased array code words for each desired outgoing angle after combining with the optimized metasurface phase map. For the downlink, the configuration includes a optimized metasurface phase map capable of focusing incoming signal strengths across a broad range of incidence angles.

To verify our proposed MetaLEO, we perform evaluations using the theoretical modeling, High Frequency Structure Simulation software (HFSS), and real-world testbed experiments in the anechoic chamber. We fabricate the prototype of our passive metasurface with 21×21 uplink elements and 22×22 downlink elements, and a transceiver antenna board containing two 1×4 antenna arrays for 20 GHz and 30 GHz, respectively. Experiments in the anechoic chamber environment validate the functionality of our proposed MetaLEO, yielding average gains of 16.57 dB in downlink and 8.32 dB in uplink compared to a 1×4 phased array, closely aligning with the simulation results.

2   Related Work

2.1   LEO satellite communication

In recent years, the demand for reliable and high-speed communication services has grown exponentially, leading to an increased interest in LEO satellite communication systems. LEO satellites have emerged as a promising solution to address the limitations of traditional geostationary (GEO) satellites, such as high latency and limited coverage in polar regions. Although the LEO satellite communication system offers many benefits, it faces several significant challenges. First and foremost, LEO satellite communication networks work on the millimeter wave frequency bands, so that the limited transmission power on the satellite antennas and severe path loss cause to the low Signal-to-Noise Ratio (SNR) of the satellite-to-Earth link limit data rates. Next, LEO satellites move rapidly, so ground stations must be able to track all satellites crossing their Field of View (FoV) simultaneously, which increases the complexity and cost of LEO ground stations.

Conventional satellite communication utilizes parabolic antennas, which face difficulties in tracking LEO constellations as they have to deal with more than one rapidly moving satellites appearing concurrently within their view and cannot implement the handovers that occur too frequently or insufficient coverage lead to undesirable latency. An alternative solution involves employing Active Electronically Scanned Aperture (AESA) antennas, also known as massive phased array antennas, which are capable of electronically modifying beams without requiring mechanical movement. However, this method necessitates a substantial quantity of antennas in order to guarantee swift and accurate tracking. As a result, costs increase due to the requirement for Radio Frequency (RF) front-end and phase controlling circuits for each individual antenna, particularly in the mmWave frequency bands. For example, Starlink ground station equipment costs \$ 600−\$ 2500. Recently, there is increased interest in improving ground station transceivers for LEO satellite systems.

2.2   Huygens metasurface

Recently, Huygens MetaSurfaces (HMSs) have gained popularity for wireless communication, as an attractive solution to alleviate the attenuation and blockage problems for wireless links. Programmable metasurfaces are capable of controlling EM waves in real-time by utilizing active elements, such as Positive Intrinsic-Negative (PIN) diodes, varactor diodes, phase changing materials, liquid crystals, and RF switches.

Arun and Balakrishnan[1] introduced a smart surface named RFocus to improve indoor Wi-Fi signal

performance, consisting of thousands of RF switches that manage the reflection or transmission of Wi-Fi signals. In comparison, Zelaya et al.[2] devised a Large Array of Vanilla Amplifiers (LAVA) to augment indoor wireless coverage. Each LAVA element contains a power sensor that detects transmissions and controls connected amplifiers. To tackle mmWave line-of-sight obstructions, mmWall[3] utilizes a reconfigurable meta-atom with two resonant rings for relaying and re-steering beams. Wall-E[4], a dual-band reconfigurable metasurface, aims to address beam alignment challenges in complex environments. Nonetheless, the active controllable components in the mmWave band come at a high price, resulting in a prohibitive cost for programmable metasurface solutions.

Passive metasurfaces consist of periodic meta-atoms with specific patterns for transmission or reflection but are limited to a single function after fabrication. Qian and Zhang[5] developed MilliMirror, a 3-D printed passive metasurface, to address mmWave blockage issues. Han and Chen[6] proposed a dual-band metasurface for S- and C- bands. However, these designs only reflect mmWave signals towards NLOS directions and lack dynamic steering, making them unsuitable for LEO scenarios. Lima et al.[7] introduced a mechanical beam steering metasurface for Ka-band satellite communication, but it cannot achieve dynamic steering using a passive metasurface alone. Studies[8, 9] consider applying metasurfaces to phased arrays to reduce costs. Distinguishing itself from previous research, our study is the first to jointly optimize metasurfaces and phased arrays, leveraging the metasurface's ability to manipulate EM wavefronts and the programmability of small phased arrays[10]. This approach results in a cost-effective, adaptive steering-supported, and RSS-enhanced transceiver system for LEO satellite communication scenarios.

3 System Design

Huygens metasurface enables precise wavefront shaping of incident EM waves through macroscopic and microscopic design. Macroscopic design involves determining and encoding phase shift profiles into metasurfaces, while microscopic design focuses on creating meta-atoms with material, structure, and geometry to achieve full 360° phase coverage and high transmission efficiency in both downlink and uplink frequency bands. This section presents the microscopic

(i.e., meta-atom) and macroscopic (i.e., phase shift profile) designs for metasurfaces.

3.1 Dual-band meta-atom design for LEO

In LEO satellite communication, our meta-atomic design must support dual-band, wide-angle, and broad-phase shift. (1) A single metasurface should support both uplink and downlink communication, with each meta-atom controlling 0°−360° phase shift independently in both frequency bands while maintaining high transmittance. This is challenging due to potential interference from coupling between uplink and downlink patterns. (2) As satellites move, the incident angle of their signals to the metasurface changes, requiring meta-atoms to support wide incident angles without affecting phase shift ability or transmittance. (3) LEO satellite systems typically use wide bands for uplink and downlink to increase link capacity, necessitating meta-atoms with consistent phase shifting and transmission capabilities across the entire frequency range.

Several existing works designed HMSs with specific copper patterns overlaid on the substrate[11]. The meta-atoms in these HMSs have electric dipole elements that induce electric currents, and these currents can also induce orthogonal magnetic currents, ultimately exciting electromagnetic resonance and achieving efficient transmission or reflection[12]. In this paper, we design specific geometries of copper patterns on the dielectric substrate and pack them closely to implement a single meta-atom for both the downlink and uplink.

Downlink pattern: We design a Jerusalem cross-shaped element designated for operation in the downlink frequency band. We choose this element pattern because cross-slot structures provide relatively complete phase control while maintaining low-loss transmission[13, 14]. The phase regulating parameters of the downlink band are L_1 and L_D, and they are tuned together and linked by the relationship $L_D = L_1/k$, where k is a constant related to the decoupling performance. This means that we can obtain different phase responses of the meta-atom by applying different L_1 parameters.

Uplink pattern: We design another Jerusalem cross element for the uplink. Note that the metasurface is composed of periodically arranged meta-atoms, so these four corners in each meta-atom remain as a kind of cross-slot structure. Similarly, the phase regulating parameters of the uplink band are L_2 and L_U. To save

space and avoid overlap with the downlink patterns, we fix L_U is a small constant (0.25 mm) and only adjust L_2 to achieve phase modulation.

Multiple layers: To enhance the transmittance and phase shift coverage for both the downlink and uplink, we employ a multi-layer structure. As illustrated in Fig. 2, layers are separated by air gaps with a height of H_2, and all layers share the same geometric design.

Considering that our metasurface is designed as a transmissive metasurface, we observe the transmittance parameter S21 to obtain the frequency response of each meta-atom design. Specifically, |S21| represents the amplitude response and ∠S21 represents the phase response. We build a meta-atom model in the Ansys HFSS 3D electromagnetic field simulator[15], as shown in Fig. 2. The simulated model includes input and output Floquet ports along its broadside direction, and the remaining four walls of the air box are assigned with Periodic Boundary Conditions (PBCs). An example of our meta-atom's frequency response of transmission amplitude is displayed in Fig. 3, when varying the downlink and uplink phase regulating parameters (i.e., L_1 and L_2). The other structure parameters are kept as default: L = 5.3 mm, k = 3, L_U = 0.1 mm, R_θ = 0°, H_2 = 2.5 mm, the permittivity of substrate (ε) is set as 2.2, and a total of 2 layers. Our results show that our closely packed meta-atom consisting of downlink and uplink patterns can support both frequency bands with maximum energy transmission.

To this end, the microscopic design is complete, we can use our macroscopic phase profile design in Sections 3.2 and 3.3 to determine the phase offset values in both the uplink and downlink of each meta-
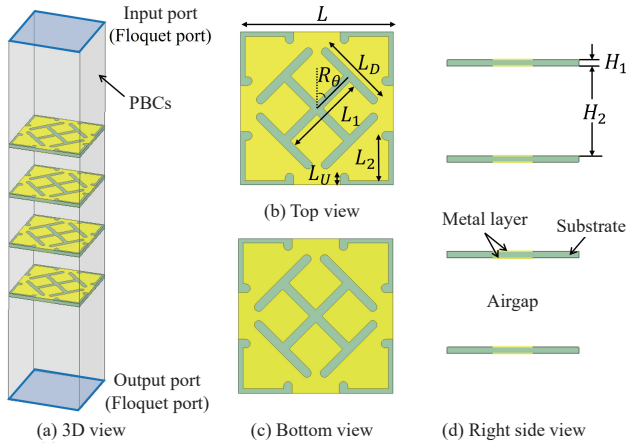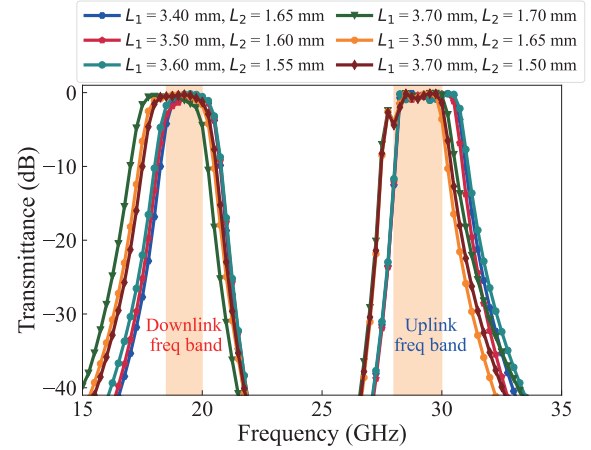

Fig. 3 Frequency response of transmission amplitude with dual-band meta-atom design, showcasing the impact of varying pattern parameters on performance in both frequency bands.

atom. To do this, we map the desired phase offset of each meta-atom to L_1 and L_2 using the curves in Figs. 4a and 5a. Then, we build a metasurface of periodically arranged meta-atoms, with desired function of controlling wavefront and radiation patterns. Our metasurface has $N \times N$ elements for downlink wavefront manipulation and $(N-1) \times (N-1)$ elements for uplink. The entire metasurface design is shown in Fig. 6.

3.2 Macroscopic design for uplink

Our objective is to develop a metasurface featuring adaptive steering for uplink, which directs EM waves from the transmission antenna towards the satellite's position. Unlike passive metasurfaces, which cannot modify their phase delay profile after fabrication, we combine phased array antenna techniques with the metasurface. We construct an optimization model to obtain the ideal metasurface phase map configuration and the codebook of phased array antennas, facilitating efficient electronic beam steering for LEO satellite communication scenarios.

3.2.1 Steering with optimized metasurface and phased array

Suppose the system must steer the beam towards the LEO satellite across a range of angles, i.e., from −40° to 40°. For each outgoing angle, we can determine the phased array beam weight to ensure proper signal steering through the metasurface.
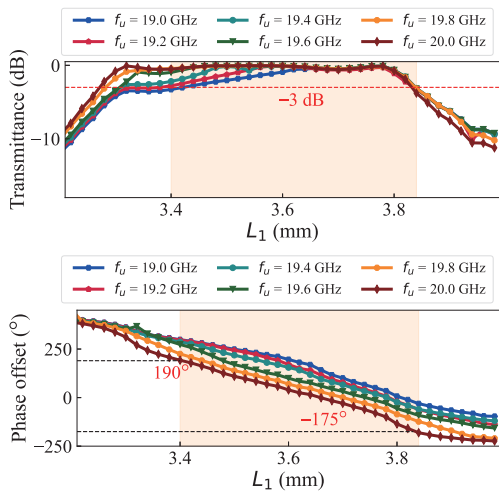
As depicted in Fig. 7, the transmitted signal x is initially radiated from the antenna array w and then traverses the wireless channel C between the antenna
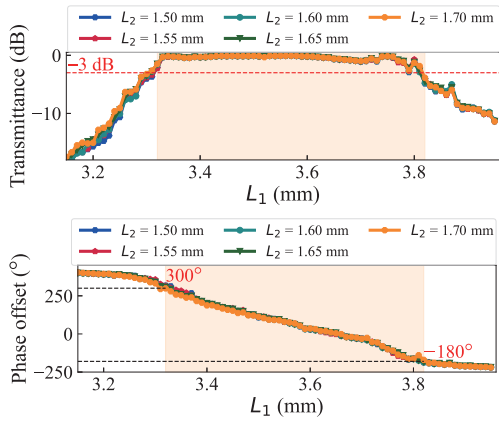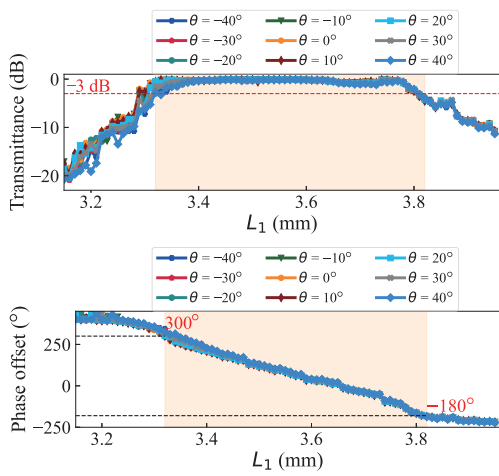
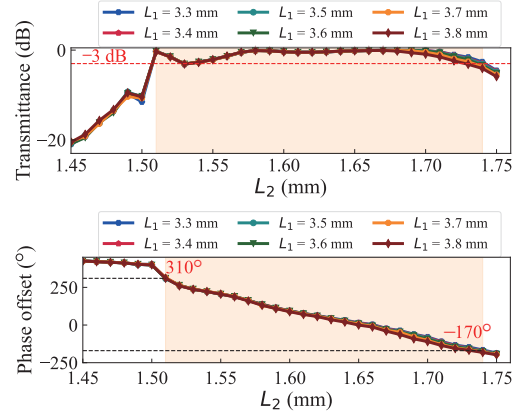**Fig. 2 Geometry of our proposed dual-band meta-atom.**

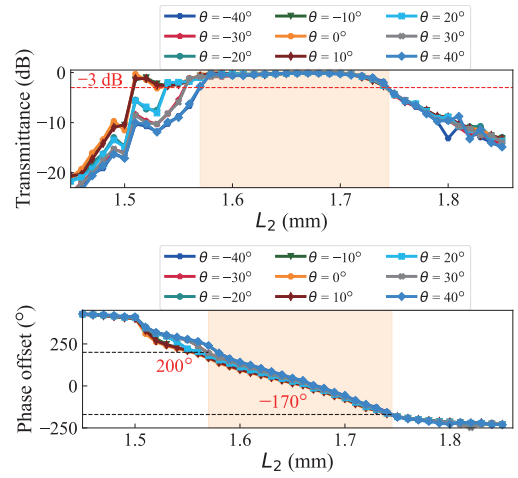(a) Transmittance and phase offsets at different L_1 parameters

(b) Transmittance and phase offsets at different incident angles

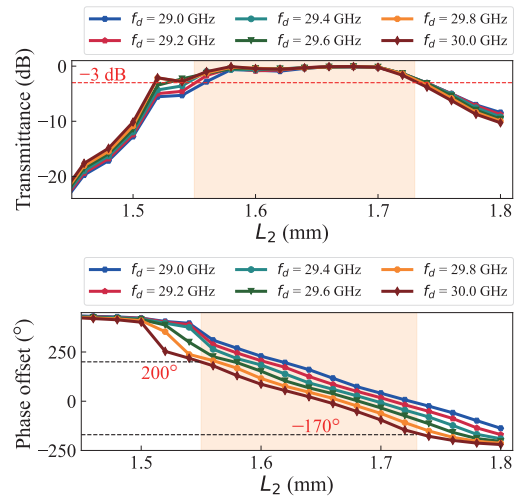(c) Transmittance and phase offsets at different uplink frequency points (f_u)

Fig. 4 Transmission amplitude and phase responses of the optimal unit cell at downlink frequency bands.

(a) Transmittance and phase offsets at different L_1 parameters

(b) Transmittance and phase offsets at different incident angles

(c) Transmittance and phase offsets at different downlink frequency points (f_d)

Fig. 5 Transmission amplitude and phase responses of the optimal unit cell at uplink frequency bands.

array and the metasurface. The element C_{ij} represents the channel response from the i-th antenna to the j-th metasurface element. Subsequently, the signal undergoes transformation by the metasurface with M
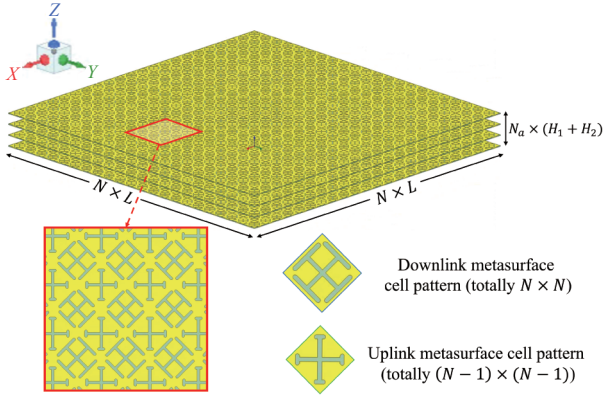
Fig. 6 Arrangement of the proposed meta-atoms to form a complete metasurface.
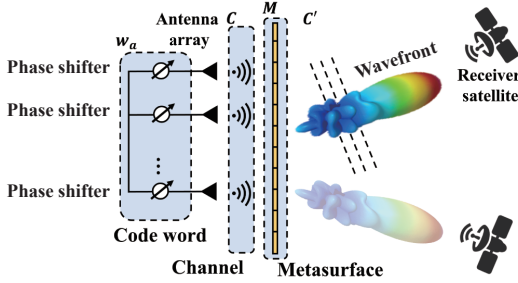

Fig. 7 Working principle of electronic steering through phased array antennas and metasurface.

phase distribution and ultimately passes through the channel between the metasurface and satellite receiver. We focus on the RSS along the steering vector C' from the metasurface to the target satellite. Thus, our aim is to maximize RSS along C', which is $R = C'MCwx$.

We aim to find a common M, i.e., phase distribution of the uplink metasurface, and the angle-determined beamforming weight matrix w_a to guarantee signal steering towards the corresponding angle a. To cover the expected range of angles, we sample angles within the range (e.g., from $-40°$ to $40°$, in step of $1°$). Our objective is to maximize the sum of the received power across all sampled angles. This can be expressed as follows:

$$\max_{M, w_a} \sum_a |C'MCw_a|^2,$$
$$\text{s.t.,} \begin{cases} |w_{ai}| \leqslant 1, & \text{for any } a, i; \\ |M_{jj}| = 1, & \text{for any } j \end{cases} \quad (1)$$

where we omit x since it is the template signal and is identical in each transmission channel. The magnitude of w_{ai} should be less than 1 due to the transmission power constraint. Additionally, the amplitude of each element on the diagonal of M should be equal to 1, as

we only consider the phase shift induced by the metasurface.

Our objective is to identify a static M and dynamic w_a for each angle a. This represents a constrained non-linear optimization problem. To solve this issue, we employ the Adam algorithm, which is a stochastic gradient descent method. To guarantee that the solution adheres to the constraints, we normalize the current M and w_a after each gradient descent iteration, ensuring their magnitudes comply with the constraints. We set the learning rate to 0.05 and the exponential decay rates for the first and second moment estimates to 0.9 and 0.999, respectively.

Benefit of our optimized metasurface: Using only 1D line phased array antennas causes directionality in only one dimension but not the other. In contrast, as seen in Figs. 8 and 9, our system combines an optimized passive metasurface with a small-sized phased array and optimized codeword to enable electronic steering and generate a highly directional beam with a small beamwidth. Our proposed system nearly matches the electronic steering function of a 2D massive phased array antennas but at a significantly lower cost, requiring only $1{\times}8$ high-frequency phase shifts instead of up to $21{\times}21$ phase shifters.

3.2.2 Supporting multiple steering angles

Until now, the emphasis has been on enabling uplink communication towards a single moving satellite with our optimized metasurface and phased array antennas. Nevertheless, in practical applications, it is more advantageous for a ground station to establish connections with multiple satellites. This approach ensures seamless transmission in situations where one satellite moves away or its signal encounters blockage, as the other satellites can provide assistance and maintain communication.

We continue to leverage the metasurface to significantly reduce the number of antennas required to achieve similar multi-beam steering performance. Specifically, given an optimized metasurface design, our objective is to derive the beamforming weights for the phased array antennas so that their outgoing waves are steered towards a given set of directions.

Based on the uplink beam steering method mentioned in Section 3.2.1, we first find the beamweight w_a for each direction a within the desired angle set S. Then, we sum up the weights for all desired directions, namely $w = \alpha \sum_{a \in S} w_a e^{j\theta_a}$, where $e^{j\theta_a}$ introduces phase delays to each beam weight w_a to
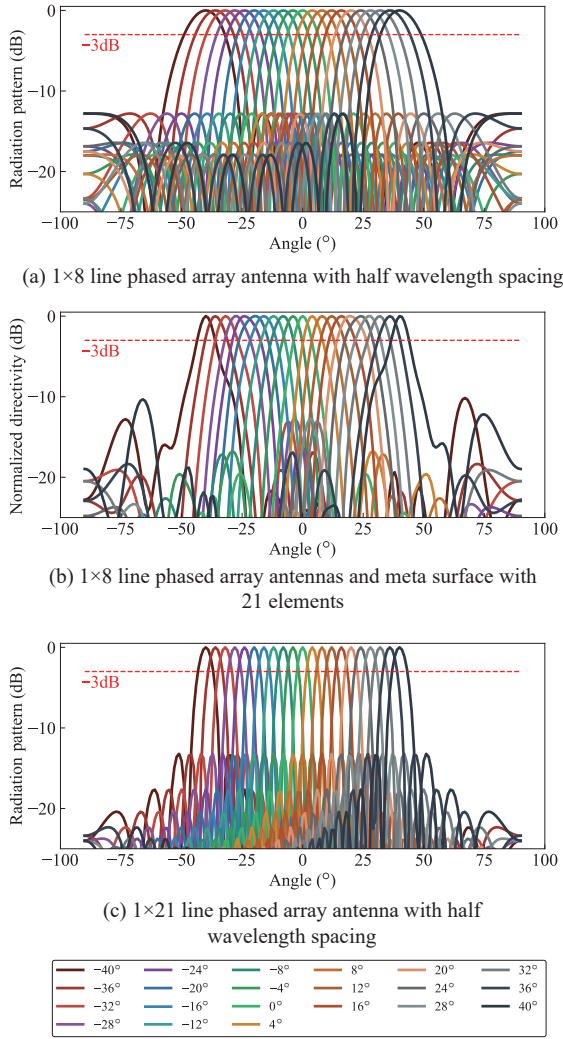
(a) 1×8 line phased array antenna with half wavelength spacing

(b) 1×8 line phased array antennas and meta surface with 21 elements

(c) 1×21 line phased array antenna with half wavelength spacing

—40°	—24°	—8°	8°	20°	32°
—36°	—20°	—4°	12°	24°	36°
—32°	—16°	0°	16°	28°	40°
—28°	—12°	4°			

Fig. 8   Resulting beam patterns for outgoing directions from −40° to 40° azimuth, with 4° increment.

achieve maximum transmission power. The term α is a power weight, that ensures that the peak power does not exceed 1. Note that we multiply the scaling factor $e^{j\theta_a}$ in each term since a beamweight is not unique, and

scaling all entries in the beamweight by a constant does not affect the beamforming direction.

To determine the appropriate scaling factor, we formulate the following optimization problem:

$$\max_{\alpha, \theta_a} w^{\mathrm{H}}w,$$

$$\text{s.t., } |w_i| \leqslant 1, \text{ for any } i \qquad (2)$$

where H represents the Hermitian transpose[16]. We solve this problem with Adam solver. The simulation results are shown as Fig. 10.

3.3   Macroscopic design for downlink

For the downlink, we need to design a focusing metasurface, so that (1) it can focus the incident plane waves from the LEO satellites to enhance RSS, and (2) it can support the focus function for the incident signals from different angles since signals transmitted by various satellites will arrive at our ground station (i.e., gateway antenna). To focus the incident waves, the discrete phase distribution on the phase gradient metasurface should satisfy the hyperbolic formation as given by Eq. (3) as follows, owing to Fermet's principle[17],

$$\phi_{x,y} = \frac{2\pi}{\lambda} \left(\sqrt{((xL)^2 + (yL)^2) + f^2} - f \right) \qquad (3)$$

where $\phi_{x,y}$ is the phase difference of the meta-atom at the point (x, y) from the center of metasurface, L is the length of each meta-atom, λ is the free-space wavelength, and f is the focal length. Figure 11a shows the lateral cut view of the radiation field after our designed focusing metasurface reshaping the incident plane waves, where the f is set as 0.02 m, metasurface consists of 22×22 elements, frequency point is set as 20 GHz, and the angle of incoming waves towards the metasurface is set as 0°. By

(a) 1×21 phased array   (b) 1×8 line array + 21×21 metasurface   (c) 21×21 phased array
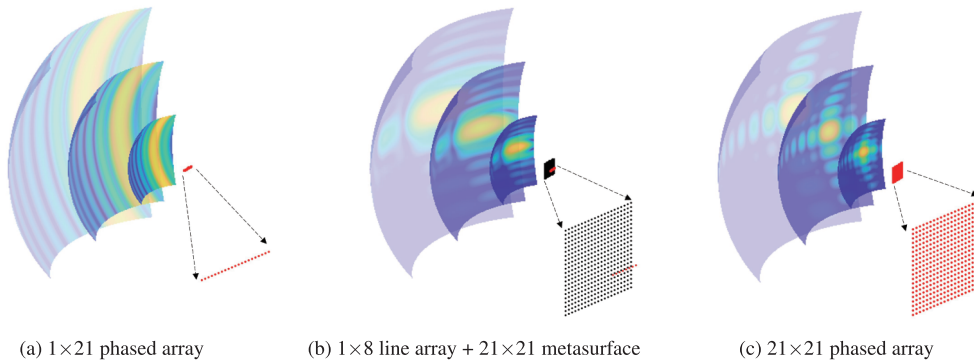
Fig. 9   Benefit of combining phased array antennas (red points) with metasurface (black points): less antennas required, more directional. These plots show the idea propagation of beam shape with different phased array and metasurface.

(a) Radiation patterns with a steering angle: −40°, 0°, and 30°.

(b) Radiation pattern with three steering angles: −40°, 0°, and 30°
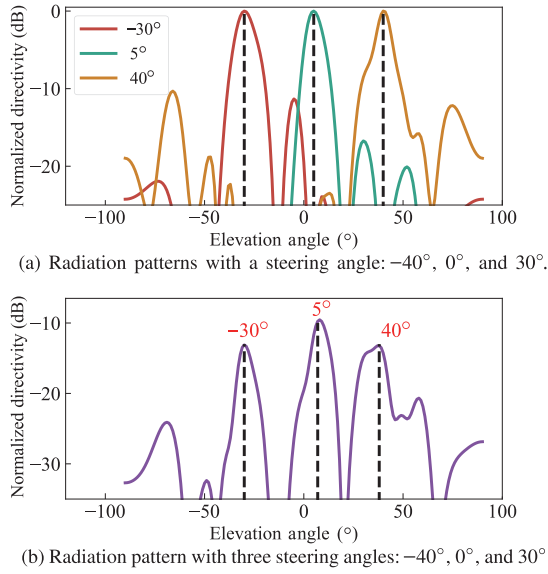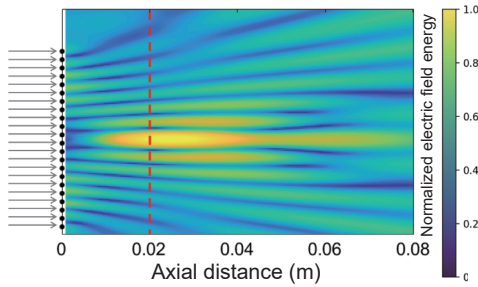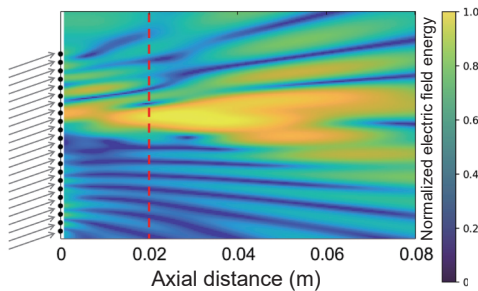
Fig. 10   Example of MetaLEO supporting multiple outgoing angles. After combining the multi-antenna excitation weights of two independent outgoing angles, we can achieve multi-transmission mode in the uplink supporting two or more outgoing directions simultaneously.

(a) Radiation field of the incident plane waves ($\theta_i = 0°$) passing through the metasurface

(b) Radiation field of the incident plane waves ($\theta_i = 20°$) passing through the metasurface

Fig. 11   Focus area is changing with the incident angles. Gray lines mean the incident EM waves, black points mean the meta-atoms in the metasurface, red dished line means the focal range.

comparing with the original incident field strength, we can conclude that metasurface with 22×22 elements

can boost the received signal strength by 23.12 dB.

To accommodate a wide incidence angle, we have designed a meta-atom structure with angle insensitivity, ensuring constant phase distribution for varying incident wave angles. However, due to slight differences in incident wavefronts, satellite signals passing through the metasurface remain focused but cause a shift in the focused region. Figure 11b displays the radiation field after our designed focusing metasurface reshapes plane waves with a 20° incident angle. The RSS gain is 21.98 dB, and the focus region shifts by 4.5 cm. We use multiple receiver antennas in a gateway antenna system placed within the range of focus area movement. Then, we employ the Maximum Ratio Combining (MRC)[18] algorithm, an optimal combiner, to maintain high RSS gain across different incident angles.

Multiple satellites receiving support: Our meta-atom, designed for wide downlink frequency bands, can focus EM waves at varying frequencies, enhancing RSS for each satellite's transmission independently. The ground station differentiates RSS-enhanced signals in the frequency domain and decodes each satellite's data. Thus, our metasurface inherently supports multi-satellite downlink reception.

4   Evaluation

In this section, we discuss the prototype implementation of our optimized passive metasurface and phased array antenna systems, along with the performance results.

4.1   Prototype implementation

We create a MetaLEO prototype to validate our design, shown in Fig. 12a. It comprises two main parts: dual-band metasurface and antenna arrays.

Metasu�race prototype: Using standard photolithographic techniques, we fabricate the metasurface on an F4BM220 sheet. The uplink metasurface has 21×21 elements, while the downlink has 22×22 elements. Phase profiles are obtained through optimization models in Sections 3.2 and 3.3, with phase distributions in Fig. 13. Our four-layer metasurface measures 12.66 cm × 12.66 cm × 1.17 cm and weighs 80.25 g.

Transceiver antenna prototype: We design two microstrip patch antenna arrays for the transmission and reception antenna prototype, fabricated on a 0.381 mm thick F4BM220 substrate, as shown in Fig. 12c.
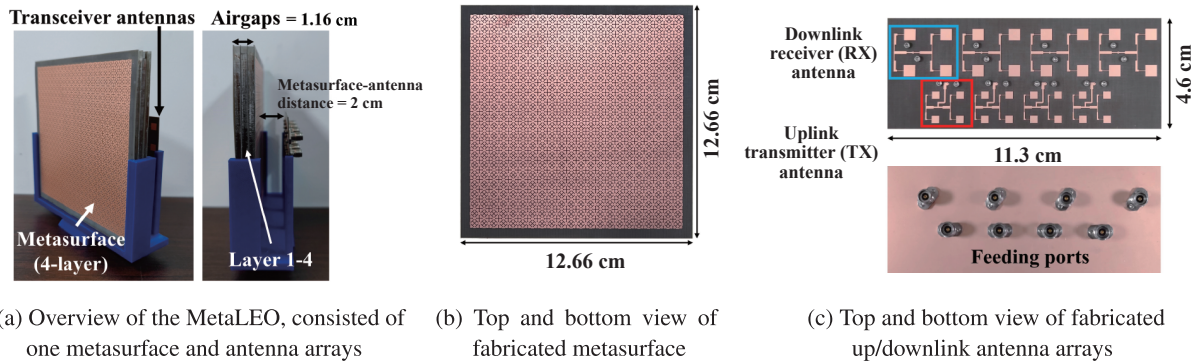
(a) Overview of the MetaLEO, consisted of one metasurface and antenna arrays

(b) Top and bottom view of fabricated metasurface

(c) Top and bottom view of fabricated up/downlink antenna arrays

Fig. 12   Photograph of the fabricated prototype of our proposed MetaLEO.
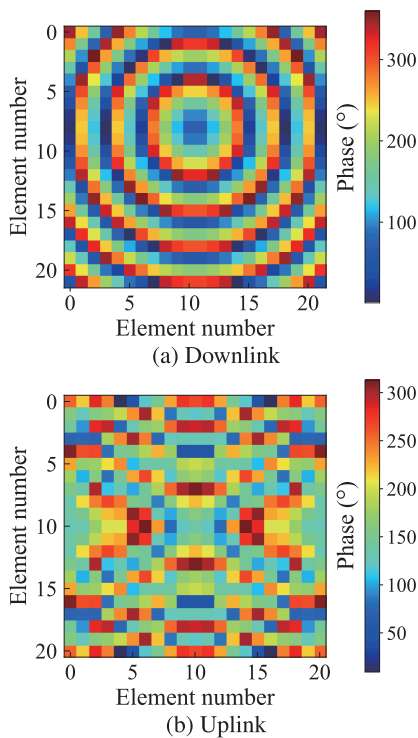

(a) Downlink

(b) Uplink

Fig. 13 Optimized desired compensating phase distributions of our designed metasurface.

4.2   Uplink performance

Beam patterns for different outgoing angles: Figure 14 compares the performance of our 1×4 linear phased array TX antennas with and without the metasurface, steering waves from 0° to 40°. Each subplot's left figure is from the theoretical simulation, while the right is from the real-world experiments conducted in the anechoic chamber. The experimental results show that measured beam patterns align well with simulations, and the TX phased array with metasurface consistently outperforms the one without. Beam width decreases upon applying the metasurface, evident in both

simulations and measurements. Measured beam pattern gain increases at the desired angle, with improvements between 6.60−8.68 dBi after adding the metasurface compared to the phased array alone, showcasing the metasurface's effectiveness in the TX array.

Impact of different frequencies: We also test the performance of our proposed system at different uplink frequencies. At 30 GHz, the gain ranges from 9.21 dBi to 11.59 dBi, between −40° and 40° between. The gains at 29−29.9 GHz is similar to the designed gain at 30 GHz. These results indicate that our metasurface can achieve a relatively wide range of radiation angles, which is sufficient for LEO satellite communications.

Steering towards multiple satellites: Figure 15 displays the performance of our system steering the outgoing beam towards two satellites at −30° and 20° simultaneously. The results show that MetaLEO can steer signals to multiple desired angles with a 1×4 phased array. Although there are sidelobes at other undesirable angles, their RSS is −8 dB lower than the main lobes, enabling reliable wireless communication.

4.3   Downlink performance

Focusing performance of metasurface and phased array: The phased array antennas can also increase RSS. We compare the performance of our system with that of the phased array on the received signal. Figure 16 shows the field intensity gain compared with a single receiving antenna for the downlink when the incident angle varies from −40° to 40°. We make the following observations. First, the results of experiments in the anechoic chamber align pretty well with that of MATLAB simulation across a wide of incident angles. Second, adding our metasurface significantly increases RSS, as we would expect. We observe an average of 16.57 dB improvement over a
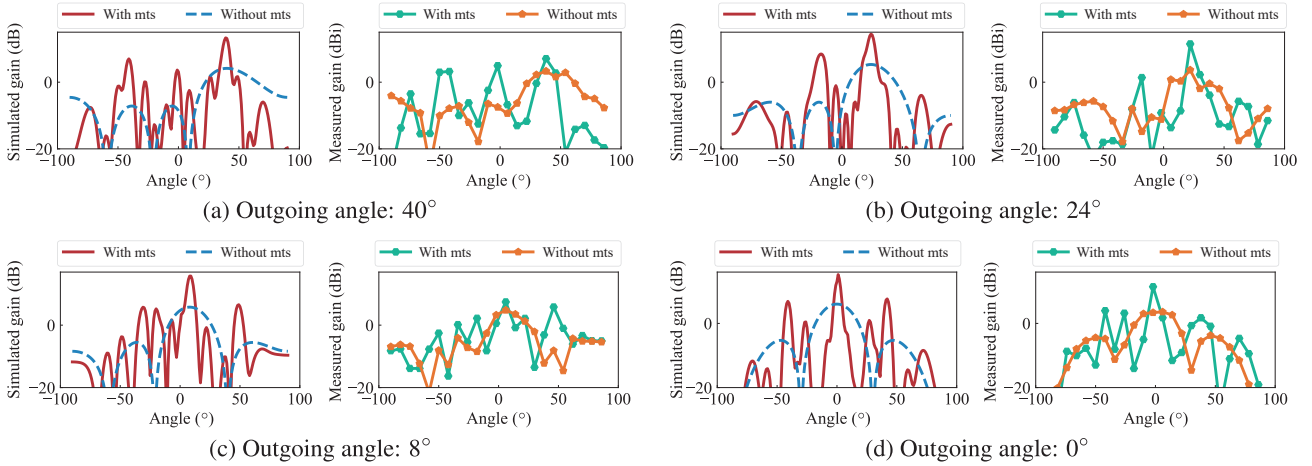
(a) Outgoing angle: 40°

(b) Outgoing angle: 24°

(c) Outgoing angle: 8°

(d) Outgoing angle: 0°

Fig. 14   Simulated and measured beam patterns for outgoing directions from 0° to 40°, 4 antennas with 2λ spacing, 21 × 21 metasurface (mts).
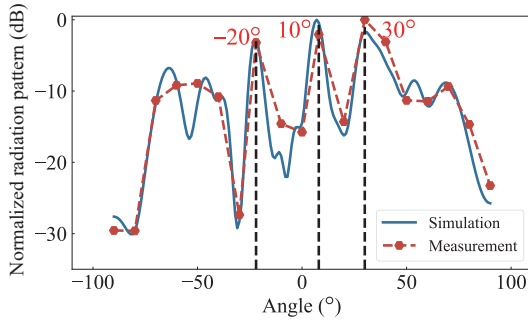

Fig. 15   Experiment results of supporting multiple outgoing angles, and three steering angles are −20°, 10°, and 30°.
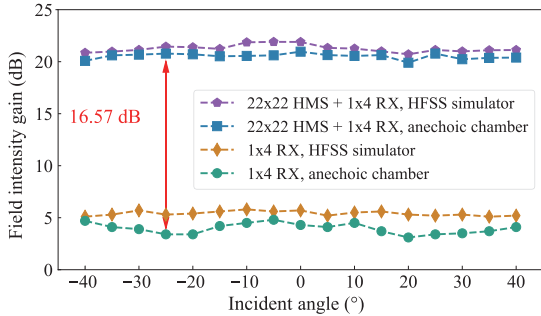

Fig. 16   Focusing performance with 22 × 22 metasurface.

1×4 phased array. This is because the metasurface is equivalent to a large-aperture antenna, which can converge EM signals from a bigger area into the receiving antenna array, resulting in a considerable RSS gain.

Impact of frequency: Figure 17 displays the field intensity gain for downlink across various incident angles and operation frequencies. Our metasurface effectively focuses incoming EM waves, enhancing RSS from −40° to 40° across a wide band in downlink. Field intensity gain remains high at around 20.4 dB for
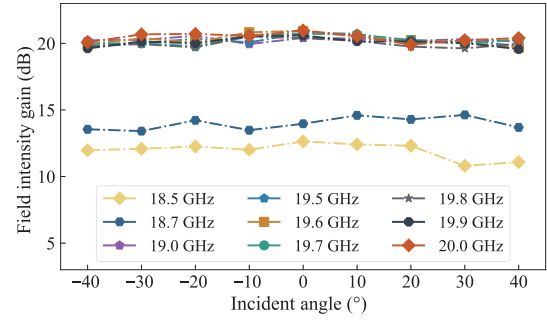

Fig. 17   Focusing performance under different frequencies

19−20 GHz, decreases to 14.3 dB at 18.7 GHz, and 12.3 dB at 18.5 GHz. A 1 GHz bandwidth suffices for downlink requirements, and the metasurface prevents amplification of noise or interference signals near the operating frequency.

Receiving from multiple satellites: We use two horn antennas to simulate two satellites transmitting signals at the same time, where each horn antenna generates EM waves at a different frequency. Then we use our patch antennas to receive the signals after passing through the metasurface. The experimental results show that the signals from different transmitters on different frequencies can independently pass through our metasurface and reach the receiver for processing without interference.

4.4   Cost comparison

Our proposed MetaLEO prototype consists of a metasurface PCB board[19] ($ 30), a 4 RX and 4 TX antenna microstrip patch array ($ 10), and four digital phase shifters[20] ($ 36) for uplink, totaling $ 140. In contrast, a phased array-only approach requires 14 × 14 antennas for uplink and 17 × 17 for downlink to
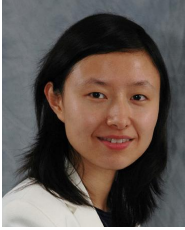
achieve comparable performance. This massive phased array transceiver includes 289 patch antennas and phase shifters, costing 73 times more. Additional cable and computational resource costs make our system a more attractive alternative for LEO satellite communication ground stations.

5 Conclusion

In this study, we firstly present a dual-frequency metasurface unit design specifically for LEO satellite communications, offering high transmittance and full phase-shift modulation across a broad range of incident angles. To achieve electronic steering performance with a passive metasurface, we employ small phased array antennas and jointly optimize the codebook of the phased array and macroscopic metasurface design. This enables dynamic beam steering and high-gain TX and RX for LEO communication. Our developed MetaLEO system prototype exhibits strength enhancements of 8.32 dB and 16.57 dB for uplink and downlink, respectively. In conclusion, our system that employs passive metasurfaces and small phased array antennas can provide an economical ground station transceiver solution for LEO satellite communication networks.

References

[1] V. Arun and H. Balakrishnan, RFocus: Beamforming using thousands of passive antennas, in *Proc. 17th USENIX Symp. Networked Systems Design and Implementation*, Santa Clara, CA, USA, 2020, pp. 1047–1061.

[2] R. I. Zelaya, W. Sussman, J. Gummeson, K. Jamieson, and W. Hu, LAVA: Fine-grained 3D indoor wireless coverage for small IoT devices, in *Proc. 2021 ACM SIGCOMM 2021 Conf.*, Virtual Event, 2021, pp. 123–136.

[3] K. W. Cho, M. H. Mazaheri, J. Gummeson, O. Abari, and K. Jamieson, mmWall: A reconfigurable metamaterial surface for mmWave networks, in *Proc. 22nd Int. Workshop on Mobile Computing Systems and Applications*, Virtual Event, 2021, pp. 119–125.

[4] K. W. Cho, Y. Ghasempour, and K. Jamieson, Towards dual-band reconfigurable metamaterial surfaces for satellite networking, arXiv preprint arXiv: 2206.14939, 2022.

[5] K. Qian, L. Yao, X. Zhang, and T. N. Ng, MilliMirror: 3D printed reflecting surface for millimeter-wave coverage expansion, in *Proc. 28th Annu. Int. Conf. Mobile Computing and Networking*, Sydney, Australia, 2022, pp. 15–28.

[6] J. Han and R. Chen, Dual-band metasurface for broadband asymmetric transmission with high efficiency, *J. Appl. Phys.*, vol. 130, no. 3, p. 034503, 2021.

[7] E. B. Lima, S. A. Matos, J. R. Costa, C. A. Fernandes, and N. J. G. Fonseca, Circular polarization wide-angle beam steering at Ka-band by in-plane translation of a plate lens antenna, *IEEE Trans. Antennas Propag.*, vol. 63, no. 12, pp. 5443–5455, 2015.

[8] R. Xu and Z. N. Chen, A compact beamsteering metasurface lens array antenna with low-cost phased array, *IEEE Trans. Antennas Propag.*, vol. 69, no. 4, pp. 1992–2002, 2021.

[9] Y. H. Lv, X. Ding, B. Z. Wang, and D. E. Anagnostou, Scanning range expansion of planar phased arrays using metasurfaces, *IEEE Trans. Antennas Propag.*, vol. 68, no. 3, pp. 1402–1410, 2020.

[10] H. Pan, L. Qiu, B. Ouyang, S. Zheng, Y. Zhang, Y. C. Chen, and G. Xue, PMSat: Optimizing passive metasurface for low earth orbit satellite communication, in *Proc. 29th Annu. Int. Conf. Mobile Computing and Networking*, Madrid, Spain, 2023, p. 43.

[11] M. Chen, M. Kim, A. M. H. Wong, and G. V. Eleftheriades, Huygens' metasurfaces from microwaves to optics: A review, *Nanophotonics*, vol. 7, no. 6, pp. 1207–1231, 2018.

[12] H. Hao, X. Ran, Y. Tang, S. Zheng, and W. Ruan, A single-layer focusing metasurface based on induced magnetism, *Prog. Electromagn. Res.*, vol. 172, pp. 77–88, 2021.

[13] L. Zhang, J. Guo, and T. Ding, Ultrathin dual-mode vortex beam generator based on anisotropic coding metasurface, *Sci. Rep.*, vol. 11, no. 1, p. 5766, 2021.

[14] A. O. Bah, P. Y. Qin, R. W. Ziolkowski, Q. Cheng, and Y. J. Guo, Realization of an ultra-thin metasurface to facilitate wide bandwidth, wide angle beam scanning, *Sci. Rep.*, vol. 8, no. 1, p. 4761, 2018.

[15] Ansys, Ansys HFSS best-in-class 3D high frequency structure simulation software, https://www.ansys.com/products/electronics/ansys-hfss, 2022.

[16] J. G. McWhirter, P. D. Baxter, T. Cooper, S. Redif, and J. Foster, An EVD algorithm for para-Hermitian polynomial matrices, *IEEE Trans. Signal Process.*, vol. 55, no. 5, pp. 2158–2169, 2007.

[17] F. Giannoni, A. Masiello, and P. Piccione, The Fermat principle in general relativity and applications, *J. Math. Phys.*, vol. 43, no. 1, pp. 563–596, 2002.

[18] Wikipedia, Maximum ratio combining, https://en.wikipedia.org/wiki/Maximal-ratio_combining, 2022.

[19] Taobao, Rogers 5880 supply ro3003 and tly-5 rogers proofing mass production in-stock high frequency plates, https://item.taobao.com/item.htm?spm=a230r.1.14.18.6fd63cbe4Lj6BA&id=669858288043&ns=1&abbucket=16#detail, 2023.

[20] pSemi, RF digital phase shifter 8-bit, 1.7–2.2 GHz, https://psemi.rfmw.com/products/detail/pe44820-psemi/554779/, 2023

Lili Qiu is an assistant managing director at Microsoft Research Asia, China, and mainly responsible for overseeing the research, as well as the collaboration with industries, universities, and research institutes. She received the PhD degree in computer science from Cornell University, USA in 2001. She is an expert in Internet and wireless networking, and worked at Microsoft Research Redmond as a researcher in the System & Networking Group in 2001−2004. In 2005, she joined University of Texas at Austin, USA, as an assistant professor at Department of Computer Science, and later, in view of her outstanding achievements in the Internet and wireless networks fields, she was promoted to a tenured professor and doctoral advisor. She is an IEEE fellow, an NAI fellow, and an ACM fellow, and also serves as the ACM SIGMOBILE chair. She was named ACM Distinguished Scientist and was a recipient of the NSF CAREER award, among many other honors. Her research interests are in Internet and wireless networking.

Hao Pan is a senior researcher at Microsoft Research Asia, Shanghai, China. He received the BEng degrees from University of Electronic Science and Technology of China, China in 2016, and the PhD degree in computer science from Shanghai Jiao Tong University, China in 2022. His research interests focus on networked systems, and span the areas of wireless communication and sensing, human-computer interaction, and computer vision.